Local SAR Prediction Errors with Variation of Electrical Properties in the Head at 7T

Muhammad Hassan Chishti[1], Zhangwei Wang[2], and Desmond T.B. Yeo[1]
[1]*GE Global Research Center, Niskayuna, New York, United States,* [2]*GE Healthcare, Waukesha, Wisconsin, United States*

Introduction: Specific Absorption Rate (SAR) is a key metric for evaluating and predicting the thermal risk to patients during RF exposure in MR scans. SAR distributions in patients are dependent on the underlying distributions of the electric field (E- field), electrical conductivity (σ), and volumetric density (ρ). The E-fields are also dependent on σ and relative permittivity (ε) of the patient. Given the variability of electrical properties (EP) of human tissue in literature [1-3], EM modeling-based methods for local SAR prediction may over- or under-estimate local SAR risk if incorrect values of EPs are used. Meng *et al*. reported that variation in electrical properties within 20% can cause peak SAR_{10g} to vary by less than 10% at 430 MHz [4]. In this work, we investigate the variation of peak SAR_{10g}, whole head average SAR, and the ratios of these two quantities with respect to variations in ε and σ in a spherical white-grey matter phantom and a human body model in a 7T transmit head coil model.

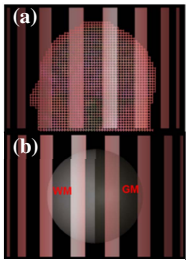

Fig. 1. (a) HBM in 7T coil (only head region shown). (b) Phantom with WM and GM

Methods:

FDTD modeling: A 16-rung high-pass birdcage head coil (dia=30.2 cm, L=21.0 cm) with RF shield (dia=37.5 cm, L=23.0 cm) was modeled and tuned loaded (spherical phantom, dia=16.4 cm, σ=0.8 S/m, ε=78.0) to 298.2 MHz using xFDTD (Remcom, State College, PA). The coil was driven in quadrature mode with four ports having equal voltage magnitude and phase values of 0°, 90°, 180°, and 270°. A spherical "brain" phantom divided into two halves (white- (σ=0.41276 S/m, ε=43.82) and grey matter (σ=0.69153 S/m, ε=60.08)), and the visible man human body model (HBM) (23 tissue types, weight: 89 kg, height: 1.77m) were used in two groups of simulations, as shown in Fig. 1. The FDTD cell size for the coil, shield, HBM and background was set to 3mm × 3mm × 3mm.

Experiments: The nominal values of ε and σ (ground truth values in our experiments) for all tissues were calculated using [5]. Experiments performed are categorized into four sets: (A) EPs of WM, GM, and CSF for HBM varied simultaneously by the same proportion, (B) EPs of WM alone varied in HBM, (C) EPs of WM and GM varied simultaneously for sphere phantom, (D) EPs of WM alone varied for sphere phantom. In each of the above four sets, (i) first only σ values are varied (nominal ε), then (ii) the ε values (nominal σ), and finally (iii) both σ and ε values are varied by ±5%, ±10%, and ±20%. A total of 74 simulations were performed on an Intel Xeon quad-core 2.13 GHz CPU with two Nvidia Quadro FX5800 GPUs. Experiments will be denoted as labeled above, e.g., "Ai" has σ variation of all tissues in HBM.

Results and Discussion: Reference (nominal) SAR results with nominal values of σ and ε are summarized in Table 1. The percentage deviation from nominal values in peak SAR_{10g}, whole head/ phantom average SAR, and SAR ratios for each of the four sets of experiments are plotted in Fig. 2. We first analyze the SAR ratios since they are normalized to the whole head average SAR power absorbed and are thus more robust to peak SAR_{10g} and WH SAR_{avg} shifts caused by changes to the coil loading induced by the variation in EP values. As σ is increased, the SAR ratio goes down for experiments B to D and slightly up for A (Fig. 2a), with the sphere (C-D) having the largest variation. As ε is increased (Fig. 2d), SAR ratios for experiments C and D increases, and remain relatively unchanged for case B, and slightly increases for case A. As σ and ε are increased concurrently (Fig. 2g), SAR ratios for case C clearly increase, and decrease for B and D. For case A, SAR ratios initially go up and show a tendency to go down with 20% increment in both σ and ε. Maximum percentage change for SAR ratio in HBM is -7.83% and occurs when both σ and ε of all three tissues is reduced by -20% (Fig. 2g). This seems to be driven by the combined effects from changing σ (Fig. 2a) and ε (Fig. 2d). Variation in ε in HBM has induced higher deviation in SAR ratio estimates compared to variation in σ. The sphere phantom has shown higher percentage change with variation in EPs and the maximum deviation is 18.39% when ε is increased by 20%. The axial and sagittal views of peak SAR_{10g} slices for HBM and phantom are shown in Fig. 3.

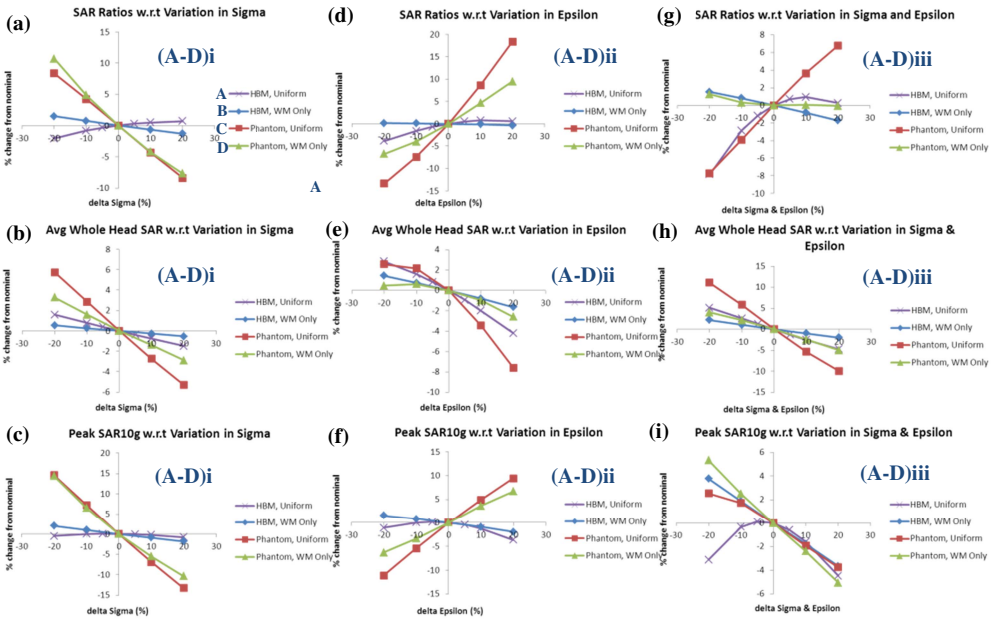

Fig. 1. SAR ratios, WH average SAR and peak SAR10g plots with variations in (**a-c**) σ (experiment labels (A-D)i, (**d-f**) ε, and (**g-i**) σ and ε.

	HBM	Phantom
Peak SAR_{10g} (mW/kg)	4.357	5.025
Whole Head/Phantom SAR Avg (mW/kg)	1.245	2.313
SAR Ratio	3.50	2.17

Table 1. SAR values for nominal σ and ε.

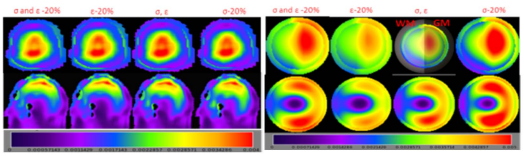

Fig. 3. SAR_{10g} maps for HBM (left) and phantom (right) where SAR ratio deviations from nominal was large.

Conclusions: Increase in σ is often associated with increased peak SAR_{10g} however the converse is observed here because the underlying E-field distribution and coil loading are likely impacted by changes in σ. In the phantom, increase in σ decreases SAR ratio while the converse is true for increase in ε. In future work, variation in the E-field distributions will be studied to better characterize the sources of the SAR ratio variability with variations in electrical properties. In our experiments with simultaneous variation of EPs in the HBM, the peak SAR_{10g} and SAR ratios were not underestimated by more than 4.48% and 7.83%, respectively (underestimating local SAR presents higher risk to patient than overestimating SAR).

References: [1] Peyman A, et al. Phys. Med. Biol. 2009; 54:227-41. [2] Bao JZ, et al. IEEE TMTT 1997; 45:1730-41. [3] Gabriel C, et al. Phys. Med. Biol. 2006; 51:6033-46. [4] Meng M, et al. IEEE TBE 2009; 56:2083-94. [5] Gabriel C, et al. Phys. Med. Biol. 1996; 41:2271-9.